# On the synchronization of banking financial indexes: a wavelet-based approach

**Wilson Silva Oliveira**[1]
**Paulo Rogério Faustino Matos**[2]
**Cristiano da Costa da Silva**[3]

## Abstract

We add to the discussion on the transmission of business cycles, by modeling worldwide banking sector indices cycle synchronization, accounting for the time-varying and frequency--specific behavior of the variables. Based on the multiple coherence, partial coherence, partial phase-difference, and partial gain, we find regions of strong and significant coherency between NAFTA partners, and in the European core: France, Germany, and the United Kingdom. Concerning such trade blocs, we also find strong performance in the period 2010-2012 in all frequencies, a period characterized by the sovereign debt crisis in some European countries.

## Keywords

Sovereign debt crisis; Trade blocs; Banking contagion.

## Resumo

Nós acrescentamos à discussão sobre a transmissão dos ciclos de negócios, modelando a sincronização dos ciclos dos índices do setor bancário mundial, levando em consideração o comportamento variante no tempo e frequência específica das variáveis. Com base na coerência múltipla, coerência parcial, diferença de fase parcial e ganho parcial, encontramos regiões de coerência forte e significativa entre os parceiros do NAFTA e no núcleo europeu: França, Alemanha e Reino Unido. Em relação a esses blocos comerciais, também encontramos forte desempenho no período 2010-2012 em todas as frequências, período caracterizado pela crise da dívida soberana em alguns países europeu.

[1] Gerente – Banco do Brasil – End.: Av. da Universidade, 2.583 – Bairro: Benfica – CEP: 60020-181. Fortaleza-CE – Brazil - E-mail: wilson_silva@bb.com.br – ORCID: https://orcid.org/0000-0001-6259-6653.

[2] Professor Associado – Universidade Federal do Ceará(CAEN/UFC) – Diretoria FEAAC. End.: Av. da Universidade, 2.486 – Bairro: Benfica – CEP: 60020-180 – Fortaleza-CE – Brazil. E-mail: paulomatos@caen.ufc.br – ORCID: https://orcid.org/0000-0002-3566-5251.

[3] Professor Adjunto – Centro de Ciências Agrárias. Universidade Federal do Ceará (CCA/UFC). Diretoria CCA - Bloco 847 – End: Av. Mister Hull, 2.977 – Bairro: Campus do Pici CEP: 60356-001 – Fortaleza-CE – Brazil – E-mail: cristiano.dacostadasilva@hotmail.com. ORCID: https://orcid.org/0000-0001-9534-5332.

Recebido: 25/09/2020. Aceito: 13/06/2022.
Editor Responsável: Dante Mendes Aldrighi

**Palavras-chave**
Crise da dívida soberana; Blocos comerciais; Contágio bancário.

**Classificação JEL**
C63; G21; O16.

## 1. Introduction

According to the extensive literature on the nature of the long-run and of short-run linkages among financial markets and their interaction, international financial integration can be seen able to increase economic efficiency and growth, but it may also influence countries' vulnerability to contagion.

Concerning the relevance and the complexity, Aharony and Swary (1983) propose distinguishing banking turmoil's episodes generated by frauds and internal irregularities from that one caused by common failures in the industry. Moreover, they also argue that the former has no contagion effect, while the latter generating spillover effect on the whole banking system by the investors' reaction. More recently, Dungey and Gajurel (2015) point out that the contagion effect on banking sector is regime dependent to economic conditions, so that when there are macro fundamentals, banking crises are overwhelmingly associated with the presence of both systematic and idiosyncratic contagion. Following Buhler and Prokopczuk (2010), banking contagion is worrying, since the dependence between banks over time is higher than other sectors of the economy. The high sensibility of the banking sector to business cycle and the rising of systematic risk in uncertain environment times reinforce the need of a system-based bank regulation, according to Meltzer (1967).

Theoretically, the reasons the reasons for worrying about this issue can be due to specific transmission channels. Kaufman (1992) suggests that an adverse shock at a bank (or banking sector of a given country) is propagated for other banks through runs. The withdrawals struggle the resources of the banks, resulting in liquidity problems and forcing up them sell assets quickly and/or to borrow funds quickly at higher interests. Moreover, even countries with unrelated economic activities can be exposed to the financial stress by international flows co-movements if they had a common bank lender. A disturbance that rising the default risk for

at least one of these countries and affects the balance sheet of the lender, restricts the services offers by this bank for all other countries (Rigobon, 2019). Kaminsky and Reinhart (2000), Kaminsky and Reinhart (2002) and Pavlova and Rigobon (2008) have examined the common lender assumption and concluded that portfolio constraints experienced by center's lenders are an important channel of transmission of financial turmoil. Finally, recent studies found that contagion of the sub-prime financial crisis ran across the Asian markets between 2007 and 2010, rising the dependence within the region (Rajwani and Kumar, 2016 and 2019).

From the empirical point view the context where spillover and contagion events occur make it harder to modelling with traditional time series tools. Rigobon (2019) indicates that the financial spillovers are accompanied with strong increases of volatility in the system, it changes the degree of misspecification on regression and increases the difficult to split the regression bias from the spillover effects. The transmission mechanism of financial shocks is highly non-linear and causes structural breaks on the volatility transmission cross-market, features that probably increases the regression bias (Jung and Maderitsch, 2014). Most of the literature has modeled transmission shocks by reduce form of generalized vector autorregression (Diebold and Yilmaz's, 2012; Akhtaruzzaman, Boubaker and Sensoy, 2021) and/or by Dynamic Conditional Correlation GARCH (Hung, 2019; Gamba-Santamaria et. al, 2017). Although these methods are effectives to deal with the drawbacks, they do not allow study the dynamic of transmission channel into different frequencies which it's important to determine the degree of persistence of them. Examining the average-lived of shocks transmission is fundamental to support political measures more effectives to reduce the systematic risk on banking sectors.

Once the motivation for the study of bank contagion is substantiated, we add to the empirical related literature, by modelling the dependence across the international banking sectors into the time-frequency domain. We are the first, to the bets of our knowledge, to use the Continuous Wavelet Transform aiming to measure the local correlation and lead/lag relationship between the international banking sector indexes over different scales (short-lived cycles, medium-lived cycles, and long-lived cycles). While applications in finance have not yet extensively utilized wavelets, there have been some interesting empirical exercises and the list is sure to grow fast. Some of the more recent closely related studies are Rua and Nunes (2009), Aguiar-Conraria and Soares (2011),

Loh (2013), Dimic et al. (2016), Lin et al. (2018), Mandler and Scharnagl (2019) and Scharnagl and Mandler (2019), Matos, Costa and da Silva (2021).

This methodology, based on Grossmann and Morlet (1984), Goupillaud et al. (1984), Torrence and Compo (1998), Torrence and Webster (1999), among other authors, is well suited to our intent because it performs the estimation of the spectral characteristics of a time-series, enabling us to study both the time-varying and frequency-specific behavior of the variables. Moreover, wavelets are mathematical functions that have advantages over traditional Fourier methods, besides improving the analysis of the non-stationary cycles on the comparison to the traditional method of understanding the trend and financial projections.

More specifically, we perform an empirical exercise aiming to test if the synchronization is statistically significant by Monte Carlo simulations. Based on this metric, we fill a dissimilarity matrix which is used to map the countries into a two-dimensional axis in terms of banking cycle synchronization. As preliminary analysis, we compare these banking cycle dissimilarities with geographical physical distances and foreign trade. In our main empirical exercise, we use cross-wavelets and wavelet-phase difference analysis to study in more detail when and at what frequencies each country is synchronized or not. Regarding the data, we use a sample of the main worldwide financial sector indices, which are comprised of the banking, insurance, and financial intermediation companies. Our cross-section considering G-2o economies is composed of financial sector indices of Australia, Brazil, Canada, Germany, France, India, Mexico, UK, USA, and Russia, covering the period from March 30, 2009, to December 31, 2013, 1255 observations. The return on these financial sector indices is stationary, heteroskedastic, leptokurtic and they are not Gaussian but rather driven by probability distribution functions as Johnson SU, Error, Hyperbolic Secant, and Laplace. According to Matos et al. (2019), such banking sector indices exhibit nonlinear and no chaotic characteristics, a sign of efficiency of the banking sector.

Summarizing our main findings, banking cycles in Australia and Russia seem independent of all the other cycles. We also find a synchronization between the main European economies: France, Germany, and the United Kingdom, highlighting the French banking cycle's lowest dissimilarity with the German cycle. This finding complements in some sense the eviden-

ce reported in Aguiar-Conraria and Soares (2011) on the role played by France and Germany, both forming the core of the Euroland, based on the wavelet analysis for industrial production. Our results suggest another pattern, a strong synchronization between Canada, the United States, and Mexico, precisely the countries that comprise the North American Free Trade Agreement (NAFTA), one of the largest trade blocs in the world. Concerning emerging economies, Brazilian and Indian banking systems are also synchronized, likely because they belong to the BRIC trade bloc. See Matos et al. (2016) for more details of integration and contagion of BRIC.

This paper is structured as the following. Section 2 describes the methodology. We analyze data in section 3. The empirical exercise is reported in section 4, while concluding remarks are offered in the fifth section.

## 2. The wavelet analysis approach[1]

### *2.1. The continuous wavelet transform*

The Fourier analysis can be considered one of the most important bases for the wavelet transform development. The central idea of Fourier analysis it's that any periodic function can be expressed by an infinite sum of trigonometric functions (Fourier transform). By defining a basis of sines and cosines of different frequencies, the Fourier Transform capture the relative importance of each frequency on the original signals. Given a time series $x(t)$, the Continuous Fourier Transform is:

$$F_x(\omega) = \int_{-\infty}^{+\infty} x(t)\, e^{-i\omega t} dt \tag{1}$$

where $\omega$ is the angular frequency and $e^{-i\omega t} = \cos(\omega t) - i\sin(\omega t)$ by the Euler's formula. In opposite of the original signal, the Fourier transform summarizes the data as a function of frequency and does not preserve information in time (Gençay *et al.*, 2001).

[1] To perform the wavelet-based results, we used the ASTollbox2018 for Matlab by M. Joana Soares and L. Aguiar-Conraria. To access: https://sites.google.com/site/aguiarconraria/joanasoares-wavelets/the-astoolbox.

The Fourier Analysis it's a powerful tool to modelling time series on frequency domain. The function is reversible, which allow back-and-forth between the original and transformed signals, and it gives an effective localization in frequency. So, we can access the power spectra of the signal, which describe the power distribution on different frequency bands. Besides the appealing of Fourier Transform to evaluate financial time series on frequency domain, the function does not allow decompose the time series into different time scales, which limit his applicability to study signals that exhibit bursts of volatility, abrupt regime changes, or non-stationarity, etc. (In and Kim, 2012). To reach a balance between time and frequency, the short-time Fourier transform (STFT) was developed to expand the transformation by frequency and time-shift, it slides a window across the time series and taking the Fourier transform of the windowed series The STFT is given by:

$$F_x^{\gamma}(\omega,\tau) = \int_{-\infty}^{+\infty} x(t)\,\gamma_{t,\omega}^{*}(t)dt \tag{2}$$

where $\gamma_{t,\omega}(t) = \gamma(t-\tau)e^{-i\omega t}$ with being an analysis window and *denotes the complex conjugate. Although the STFT provides the time-localized frequency information for situations in which frequency components of a signal vary over time, the constant length window used by STFT results in a transform which is limited by the Heisenberg uncertainty principle. It means that is impossible both measures the exact frequency and exact time of occurrence of this frequency in a signal (Rua, 2012). So, the drawback of STFT is that is apply fixed length window in the signal processing, which results in a uniform partition of time-frequency space, have not been able to capture events when they happen to fall within the width of the window (Gençay *et al.*, 2001).

To resolve that problem, the Wavelet transform has three additional features over Fourier transform (In and Kim, 2013): i) it can decompose the data into several time scales instead of the frequency domain (which allow us to investigate the behavior of a signal over various time scales); ii) it uses local base functions that adjust the window width to deal with different frequencies (this enables a more flexible approach to deal with high and low frequency components) and iii) it allows to work with non-stationary data. The latter feature is especially important to examine financial time series, once that heteroskedasticity, sudden regime shifts, structural breaks at unknown time points are common pattern trough the financial cycle paths.

Given a time series $x(t)$, the continuous wavelet transform (CWT) is defined as:

$$W_x(\tau, s) = \int_{-\infty}^{+\infty} x(t)\, \psi^*_{\tau,s}(t) dt \tag{3}$$

where * denotes the complex conjugate, $\tau$ determines the position, $\psi_{\tau,s}$ is the scaling factor and  is the basis function suited to scale and shift the original signal, which allows the decomposition of the time series both in space and scale (Farge, 1992). To capture the high and low frequencies of the signal, it's utilized a mother wavelet that is stretched and shifted (Francis and Kim, 2012):

$$\psi_{\tau,s}(t) = \frac{1}{\sqrt{s}} \psi\left(\frac{t-\tau}{s}\right) \tag{4}$$

The factor $1/\sqrt{s}$ is added to guarantee preservation of the unit energy ($\|\psi_{\tau,s}\| = 1$). Low scales are captured rapidly changing detail generating a compressed wavelet ($|s| < 1$), capturing high frequencies movements, and high scales capture slowly changing features ($|s| > 1$), or low frequencies movements (Rua, 2012). So, the CWT can be defined by:

$$W_x(\tau, s) = \int_{-\infty}^{+\infty} x(t) \frac{1}{\sqrt{s}} \psi\left(\frac{t-\tau}{s}\right) dt \tag{5}$$

The basis function $\psi_{\tau,s}$ must obey some criteria, such as:

i) Admissibility: for an integrable function, it means that its average should be zero and the function need be localized in both time and frequency space. where $H(\omega)$ is the Fourier transform of frequency $\omega$. It's a necessary condition to satisfy the Dialect condition, which ensures that $\lim_{\omega \to 0} H(\omega) = 0$. Hence, the first condition of a wavelet function is $\int_{-\infty}^{+\infty} \psi(t) dt = 0$.

   If the energy of a function is defined as the squared function integrated over its domain, the second condition is that the wavelet function has unit energy ($\int_{-\infty}^{+\infty} |\psi(t)|^2 dt = 1$).

ii) Similarity: the scale decomposition should be obtained by the translation and dilation of only one wavelet mother function. This dilation procedure allows an optimal compromise in view of the uncertainty principle: The wavelet transform gives very good spatial resolution in the small scales and very good scale resolution in the large scales (Farge, 1992).

iii) Invertibility: Once that the energy of the original signal is preserved by the wavelet transform if the admissibility condition is satisfied, we have $\int_{-\infty}^{+\infty}|x(t)|^2dt = \frac{1}{C_\Psi}\int_{-\infty}^{+\infty}\int_{-\infty}^{+\infty}|W_x(\tau,s)|^2\frac{d\tau ds}{s^2}$. Hence, there should be at least one reconstruction formula for recovering the signal exactly from its wavelet coefficients and for allowing the computation of energy or other invariants directly from them.

iv) Regularity: The wavelet should be concentrated one some finite spatial domain and be sufficiently regular.

v) Vanishing moments: The wavelet should have some vanishing high-order moments. This requirement allows the study of its high-order fluctuations and possible singularities in some high-order derivatives. It means that scale function is smoother.

There are many options of wavelet mother functions to select, which includes Daubechies, Haar, Mexican Hat, Morlet and Meyer wavelets. Aguiar-Conraria and Soares (2011) highlight the importance of that choice and suggest picked up an analytic wavelet to study the synchronism between oscillatory signals because its corresponding transform contains information on both amplitude and phase, providing an estimate of the instantaneous amplitude and instantaneous phase of the signal in the neighboring of each time/scale location $(\tau, s)$. On subset of analytic wavelet, the Morlet wavelet mother is the most popular alternative because some properties, which is given by:

$$\psi_{\omega_0}(t) = \pi^{-1/4}e^{i\omega_o t}e^{-t^2/2} \tag{6}$$

where the non-dimensional frequency $\omega_0$ is set $\omega_0 = 6$ to satisfy the admissibility condition (Torrence and Compo, 1998). As the wavelet transform decomposes the original signal in a time-scale domain, which put us the necessity to convert scale into frequency. Lilly and Olhede (2009) points that this conversion can be made by associate the wavelet $\psi_{\tau,s}$ with one of three special frequencies (the peak frequency, the energy function, or the central instantaneous frequency), by using the formula $\omega(s) = \frac{\omega_\psi}{s}$, where $\omega_\psi$ denotes any of the three angular special frequency.

By the usual "Fourier" frequency (cycles per unit time) we have that $f(s) = \frac{\omega_\psi}{2\pi s}$. In this sense, the Morlet wavelet is an ideal alternative becau-

se it provides us a unique relation between frequency and scale (the peak frequency, the energy frequency and the central instantaneous frequency are all equal) which makes it easier the conversion from scales to frequencies. The choice of $\omega_0 = 6$ give us a conversion ratio equal $f = \frac{6}{2\pi s} \approx \frac{1}{s}$, that direct correspondence between scale and frequency is ideal to simplify an effective interpretation of the results.

Finally, because the CWT is applied on finite-length time series, border distortions will occur due the fact that values of the transform at the beginning and the end of the sample are imprecisely computed, which involve artificial padding on the extremes of the sample (the most common is set zero to extend the time series). As larger scales decrease the amplitude near the edges as more zeroes enter the analysis (Torrence and Compo, 1998), the region that suffers from these edge effects is function of $s$. The Cone of Influence (COI) is the region of the wavelet spectrum in which edge effects become important by a factor of $e^{-2}$. In the case of the Morlet wavelet this is given by $\sqrt{2}s$.

### *2.2. Wavelet tools*

The first wavelet measure that we will present it's the wavelet power spectrum (WPS), which reports the variance distribution of the original time series $x(t)$ around the time-scale (or time-frequency) plane. Following Torrence and Compo (1998) we define the WPS by:

$$WPS_x(\tau, s) = |W_x(\tau, s)|^2 \tag{7}$$

To compare the oscillation in energy among a range of bands (or frequency) we define the Global Wavelet Power Spectrum (GPWS), which takes the average of wavelet power spectrum over all times (Aguiar-Conraria and Soares, 2011):

$$GWPS_x(\tau, s) = \int_{-\infty}^{+\infty} |W_x(\tau, s)|^2 d\tau \tag{8}$$

To study the dependencies between two original time series $x(t)$ and $y(t)$ in time-scale/frequency plane, Torrence and Webster (1999) were the first to define the wavelet coherence. The measure that is associated

to the cross-wavelet spectrum (XWT), which in turn can be derived by (Torrence and Compo, 1998):

$$W_{xy}(\tau, s) = W_x(\tau, s)W_y^*(\tau, s) \tag{9}$$

where $W_x(.)$ and $W_y(.)$ are continuous wavelet transform of $x(t)$ and $y(t)$, respectively, and * denotes the conjugates complex. As the cross-wavelet transform is complex, we can express the XWT as $\left|W_{x,y}(\tau, s)\right|$. It computes the local covariance between two signals at each scale. The squared wavelet coherence is given by the squared of the wavelet cross-spectrum normalized by the individual power spectra. Following Torrence and Webster (1999) the squared wavelet coherence is denoted as:

$$R^2(\tau, s) = \frac{\left|S\left(s^{-1}W_{x,y}(\tau, s)\right)\right|^2}{S(s^{-1}W_x(\tau, s)^2)S\left(s^{-1}W_y(\tau, s)^2\right)} \tag{10}$$

where $S(.)$ expresses a smoothing operator in both time and scale, $s^{-1}$ is a normalization fator ensuring the conversion to an energy density. Torrence and Webster (1999) notes that in numerator of the squared wavelet coherence, both the real and imaginary parts of the cross-wavelet transform are smoothed separately before taking the absolute value, while the smoothing operator is taking on square of the wavelet power spectra in denominator. By these definitions, it's ensured that $0 \leq R^2 \leq 1$.

Hence, the main advantage of the wavelet coherence on XWT is the common measure unit to examine several combinations of signals. Torrence and Compo (1999) reveals that once the wavelet transforms conserves variance, the wavelet coherence is a good representation of the normalized covariance between two-time series, where the closer to zero (one) the coherence, the weaker (stronger) the local correlation between the time-series. The wavelet coherence has not theoretical distribution known, hence we follow the approach of Aguiar-Conraria (2011) and Torrence and Compo (1998) deriving the confidence interval using Monte Carlo methods.

Although the wavelet coherence computes the degree of local linear correlation between two signals, it isn't reveals patterns of lead-lag relationship neither if the movements are positives or negatives. To deal with these limitations, the phase-difference is commonly used to examine the delays

in the flutuactions between the two time-series. Following Torrence and Webster (1999) we define the phase difference as:

$$\phi_{xy}(\tau,s) = \tan^{-1}\left(\frac{\Im\left\{S\left(s^{-1}W_{x,y}(\tau,s)\right)\right\}}{\Re\left\{S\left(s^{-1}W_{x,y}(\tau,s)\right)\right\}}\right) \tag{11}$$

Where the smoothed real ($\Re$) and imaginary ($\Im$) parts should already be calculated in the wavelet coherence function. Both $R^2(\tau,s)$ and $\phi_{xy}(\tau,s)$ are functions of the position index ($\tau$) and scale ($s$). We also need the information on the signs of each part to completely determine the value of $\phi_{xy}\epsilon[-\pi,\pi]$. A phase-difference of zero indicates that the time-series move together at the specified frequency. If $\phi_{xy}\epsilon\left(0,\frac{\pi}{2}\right)$ the series move in phase, but the time-series $y$ leads $x$, while if $\phi_{xy}\epsilon\left(-\frac{\pi}{2},0\right)$ then it is that is leading. A phase-difference of $\phi_{xy} = \pm\pi$ indicates an anti-phase relation. Finally, if $\phi_{xy}\epsilon\left(\frac{\pi}{2},\pi\right)$, then $x$ is leading and time-series $y$ is leading if $\phi_{xy}\epsilon\left(-\pi,-\frac{\pi}{2}\right)$.

### *2.3. Wavelet spectra distance matrix*

Aguiar-Conraria and Soares (2011) developed a metric to measure the distance (dissimilarity) between the wavelet transforms of pairs of time series, such two $FxT$ wavelet transforms ($W_x$ and $W_y$). The authors use the singular value decomposition (SVD) of a matrix $W_x(\tau,s)W_y^*(\tau,s)$ to focus on the common high-power time-frequency regions. The method extracts components that maximize covariances of the pair of given wavelet spectra with the first component being the most important common patterns between as $W_x(\tau,s)$ and $W_y(\tau,s)$.

Given the SVD we compute the $K$ most relevant vectors – the leading patterns $l_x^k$ and $l_y^k$; $k = 1,..,K$; and singular vectors, $u_x^k$ and $u_y^k$; $k = 1,..,K$, with $K < F$ – which will approximately reconstruct the original matrices: $W_x \approx \sum_{k=1}^{K} u_x^k l_x^k$ and : $W_y \approx \sum_{k=1}^{K} u_y^k l_y^k$ (Aguiar-Conraria, 2013).

To measure a distance between two wavelet spectra reduced to a few components we need to measure the angle between each pair of corresponding

segments, defined by the consecutive points of the two vectors, ant take the mean of these values. As the components of lading vectors and leading patterns are complex numbers, we follow Aguiar-Conraria and Soares (2011) we use the Hermitian approach to define the angle of a complex vector space. As the Hermitian inner product of two complex vectors $\boldsymbol{a}$ and $\boldsymbol{b}$ is defined by $\langle \boldsymbol{a}, \boldsymbol{b} \rangle_C = \boldsymbol{a}^* \boldsymbol{b}$ and the norm is given by $||\boldsymbol{a}|| = \sqrt{\langle \boldsymbol{a}, \boldsymbol{a} \rangle_C}$, the Hermitian angle between the complex vectors $\boldsymbol{a}$ and $\boldsymbol{b}$ is determined by the formula:

$$\cos(\Theta_H) = \frac{|\langle \boldsymbol{a}, \boldsymbol{b} \rangle_C|}{||a||||b||}, \Theta_H \in \left[0, \frac{\pi}{2}\right]$$

and the distance between two-vectors $\boldsymbol{p} = (p_1, \cdot, \cdot p_m)$ and $\boldsymbol{q} = (q_1, \cdot, \cdot q_m)$ with components in is defined by:

$$d(\boldsymbol{p}, \boldsymbol{q}) = \frac{1}{M-1} \sum_{i=1}^{M} \Theta_H(\boldsymbol{s_i^p}, \boldsymbol{s_i^q})$$

where the $ith$ segment $\boldsymbol{s_i^p}$ two-vectors $\boldsymbol{s_i^p} \coloneqq (i+1, p_{i+1}) - (i, p_i) = (1, p_{i+1} - p_i)$

Hence, the wavelet spectra distance between $W_x$ and $W_y$ is computed as:

$$d(W_x, W_y) = \frac{\sum_{k=1}^{K} \sigma_k^2 \left[ d(\boldsymbol{l}_x^k, \boldsymbol{l}_y^k) + d(\boldsymbol{u_k}, \boldsymbol{u_v}) \right]}{\sum_{k=1}^{K} \sigma_k^2}$$

where $\sigma_k^2$ are the weighs equal to the squared covariance by each axis.

### *2.4. Multivariate tools*

To capture the interdependence and/or causality between multiple time series, following Aguiar-Conraria and Soares (2014) and Aguiar-Conraria et al. (2018) we use high-order wavelet tools which allow us to investigate the dependency of one time series upon a set of other time series (multiple wavelet coherency) on the time-frequency plane as well to examine the co-movements between two time-series after controlling the oscillations of a subset of time series (partial wavelet coherency, partial phase-difference and partial wavelet gain) on the time-frequency plane.

Given a set of $p$ time series $(x_1, x_2, .., x_p)$ with $p > 2$ and $x_i = \{x_{i_n}, n = 0, .., T-1\}$ to compute multiple and partial wavelet measures is necessary to perform a smoothing operation on the cross-spectra. Let $S_{ij}$ be the smoothed version of the cross-wavelet spectrum between the time series $x_i$ and $x_j$ ($S_{ij} = S(W_{ij})$ and $\mathcal{L} = \left(S_{ij}\right)_{i,j=1}^{p}$ denote the $pxp$ matrix of all the smoothed cross-wavelet spectra. It's important observe that this matrix is function of specific combination $(\tau, s)$ at which the spectra are being computed and it's a Hermitian matrix ($\mathcal{L} = \mathcal{L}^H$) where the symbol $H$ denotes conjugate transpose. So, $S_{ij} = S_{ji}^*$, $\forall\, i \neq j$ and $S_{ii} = S(|W_i|^2)$ is a real (positive) number $\forall i$. The *squared multiple wavelet coherency* between the series $\boldsymbol{x_1}$ and all the other series $\boldsymbol{x_2, .., x_p}$ is given by:

$$R^2_{1(2..p)} = 1 - \frac{\mathcal{L}^d}{S_{11}\mathcal{L}^d_{11}}$$

where $d$ denotes the determinant of the matrix, and $\mathcal{L}^d_{ij}$ denotes the cofactor of the element in position $(i, j)$, i.e. $\mathcal{L}^d_{ij} = (-1)^{i+j} det\mathcal{L}^j_i$, where $det\mathcal{L}^j_i$ denotes the determinant of the submatrix obtained by crossing out the row $i$ and column $j$ of $\mathcal{L}$ to convert it to $\mathcal{L}_{ij}$.

The *complex partial wavelet coherency* of $x_1$ and $x_j$ $(2 \leq j \leq p)$ allowing for all the other series will be computed by:

$$\varrho_{1j.q_j} = -\frac{\mathcal{L}^d_{j1}}{\sqrt{\mathcal{L}^d_{11}}\sqrt{\mathcal{L}^d_{jj}}}$$

The *partial wavelet coherency* of $x_1$ and $x_j$ allowing for all the other series, is denoted by:

$$R_{1\ j.q_j} = \frac{\left|\mathcal{L}^d_{j1}\right|}{\sqrt{\mathcal{L}^d_{11}}\sqrt{\mathcal{L}^d_{jj}}}$$

And the *squared partial wavelet coherency* of $x_1$ and $x_j$ is simply the square of $R_{1\ j.q_j}$.

Since that the complex partial wavelet coherency measures the local correlation between the time series $x_1$ and $x_j$ after controlling the influence

of all the other time series ($x_i; i = 2,..,p \; and \; i \neq j$), Aguiar-Conraria and Soares (2018) define the *partial phase-difference* of $x_1$ over $x_j$ as:

$$\phi_{1j.q_j} = \tan^{-1}\left(\frac{\Im\left(\varrho_{1j.q_j}\right)}{\Re\left(\varrho_{1j.q_j}\right)}\right)$$

Following Aguiar-Conraria et al. (2018) we define the *complex partial wavelet gain* of the time-series $x_1$ over the time series $x_j$ as follow:

$$\mathcal{G}_{1j.q_j} = -\frac{\mathcal{L}_{j1}^d}{\mathcal{L}_{11}^d}$$

And the *partial wavelet gain* is computed by the modulus of the *complex partial wavelet gain*. Then:

$$G_{1j.q_j} = \frac{\left|\mathcal{L}_{j1}^d\right|}{\mathcal{L}_{11}^d}$$

Note that the *partial wavelet gain* provides us a measure similar to the (modulus) coefficient of a multiple linear regression of $x_1$ against the explanatory variables $x_2,,,x_p$ (for $j = 2,..,p$) at each time and frequency.

Aguiar-Conraria et al. (2018) highlights that these measures can be specified by wavelet complex coherencies. Consider a matrix $\mathfrak{L} = \left(\varrho_{ij}\right)_{i,j=1}^{P}$ of all the complex wavelet coherencies $\varrho_{ij}$. Hence, the multiple wavelet coherency can be computed as:

$$R_{1(2..p)}^2 = 1 - \frac{\mathfrak{L}^d}{\mathfrak{L}_{11}^d}$$

The complex partial wavelet coherency $\varrho_{1j.q_j}$ and the partial wavelet coherency $R_{1j.q_j}$ are denoted, respectively, by:

$$\varrho_{1j.q_j} = -\frac{\mathfrak{L}_{j1}^d}{\sqrt{\mathfrak{L}_{11}^d}\sqrt{\mathfrak{L}_{jj}^d}} \quad \text{and} \quad R_{1j.q_j} = \frac{\left|\mathfrak{L}_{j1}^d\right|}{\sqrt{\mathfrak{L}_{11}^d}\sqrt{\mathfrak{L}_{jj}^d}}$$

Finally, the complex partial wavelet gain $\mathcal{g}_{1j.q_j}$ and the partial wavelet gain $G_{1j.q_j}$, respectively, by:

$$\mathcal{g}_{1j.q_j} = -\frac{\Omega^d_{j1}}{\Omega^d_{11}}\frac{\sigma_1}{\sigma_j} \quad \text{and} \quad G_{1j.q_j} = \frac{|\Omega^d_{j1}|}{\Omega^d_{11}}\frac{\sigma_1}{\sigma_j}$$

## 3. Data and descriptive statistics

### *3.1. Summary statistics*

Major market indices are well known and they use to be composed of stocks of companies from several sectors of the economy. However, by incorporating all these companies, we lose the power of explaining a particular segment of the market. Aiming to deal with this issue, we observe the appearance of sectoral indices, with a proposal to complement the general market indices and providing summary information about a specific sector of the economy. We implement an empirical exercise applying wavelet analysis in a sample of the main worldwide financial sector indices of G20 economies. This sector consists of banks, insurance companies, and other financial intermediation companies and its idiosyncrasies make it more likely to be influenced by contagion and integration. Banks, insurance companies, and other financial companies in major economies are often strongly connected, with interdependence in the short and long term.

We report in Table 1 a basic description of such financial indices.

**Table 1 - Main worldwide financial sector indices**

| Country | Financial Sector Index | Continent | Position in the ranking (GDP, 2013) |
|---|---|---|---|
| Germany | DAX All Banks | Europe | 4th |
| Australia | ASX 200 Financials | Oceania | 12th |
| Brazil | IFNC | South America | 7th |
| Canada | TSX Financials | North America | 11th |
| United States of America | KBW Bank | North America | 1st |
| France | CAC financials | Europe | 5th |
| India | CNX Finance | Asia | 10th |
| Mexico | BMV | North America | 15th |
| United Kingdom | NMX 8350 | Europe | 6th |
| Russia | Moscow Exchange Financials Index | Europe | 9th |

In principle, whenever econometric or statistical tests are performed, it is preferable to employ a large data set either in the time-series ($T$) or the cross-sectional dimension ($N$). When working with the worldwide financial sector indices, we have to deal with the trade-off between $T$ and $N$. So, in terms of sample size, the main limitation for the time-series span used here is the appearance of this sectorial index across countries and the availability of a time series sufficiently extensive, at least one thousand daily observations, i.e., approximately four years. Aiming to have a balanced database, we adjust data series to make these calendars uniform, since the countries have different calendars in terms of working days. The criterion is to use any day that was a working day in any of the economies, aiming to deal with the differences due to the holidays between the markets located on five continents, with a greater presence of European and North American countries. Unfortunately, the relevant financial markets, such as Japanese or Chinese, or do not provide time series of its respective sectorial indices or these series are very recent.

Figure 1 shows the cumulative gross return on the financial sector indices in terms of the local investor´s currency. Table 2 reports summary statistics and in Table 3, we report pairwise correlations.

We can highlight volatility clusters and higher oscillations, mainly between 2011 and 2012, a period characterized by the sovereign debt crisis in some European countries. The country whose index has the highest cumulative gain in the period in India, with 189%, while DAX All banks in Germany have the worst cumulative gain, only 26%, and the highest drawdown among these indices, 64%. TSX Financials in Canada is the smoothest index considering all volatility measures used here. Its semivariance is only 0.73%, for instance. All series are leptokurtic with a higher intensity for CNX Finance in India, suggesting the frequency of occurring large losses. These skewness and kurtosis are strong evidence that the series does not follow a Gaussian distribution.

A simple but intuitive statistic that signals the expected results in terms of synchronization consists of the correlation, reported in Table 3. It is possible to observe on the one hand, that India and Australia are the banking systems that present less synergy with the others. The lowest correlation observed is between Australia and the United States, 0.14. On the other hand, the German and French banking indices are highlighted because they present the highest values of correlation with the indices of

the other countries. The correlation between them is the highest reported, 0.88. In terms of blocs, Mexico, Canada, and the United States share high correlations ranging from 0.58 to 0.69. We also find high correlations for the three major European economies, whose correlations range from 0.73 to 0.88.

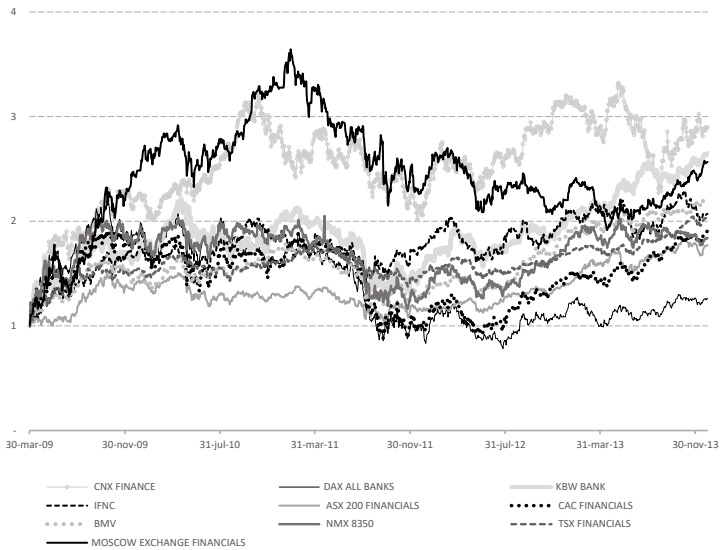


**Fig. 1 - Cumulative gross returns on main worldwide financial sector indices [a,b]**

[a] This figure plots the nominal net return on financial sector index in terms of the local investor´s currency, based on the daily time series for the end-of-day quote, during the period from March 30, 2009, to December 31, 2013. [b] Data source: Bloomberg.

**Table 2 - Statistics of series of returns on main worldwide financial sector indices (March 30, 2009, to December 31, 2013. Data source: Bloomberg).**

| Statistics | CNX Finance (India) | DAX All Bankx (Germany) | KBW Bank (USA) | IFNC (Brazil) | ASX 200 Financials (Australia) | CAC Financials (France) | BMV (Mexico) | NMX 8350 (U. K.) | TSX Financials (Canada) | Moscow Exchange Financial Index (Russia) |
|---|---|---|---|---|---|---|---|---|---|---|
| Gain | | | | | | | | | | |
| Mean | 0.10% | 0.04% | 0.10% | 0.07% | 0.05% | 0.08% | 0.07% | 0.07% | 0.06% | 0.09% |
| Cumulative | 189.57% | 26.29% | 164.76% | 107.04% | 77.17% | 91.30% | 121.28% | 84.29% | 104.28% | 156.61% |
| Risk | | | | | | | | | | |
| S. D. | 1.70% | 2.09% | 2.12% | 1.43% | 1.17% | 2.16% | 1.28% | 1.82% | 1.03% | 1.70% |
| Semivariance | 1.12% | 1.46% | 1.43% | 1.00% | 0.82% | 1.49% | 0.92% | 1.22% | 0.73% | 1.21% |
| Drawdown | 37.60% | 64.27% | 41.93% | 32.09% | 30.58% | 53.98% | 33.88% | 43.55% | 22.05% | 47.43% |
| Other moments | | | | | | | | | | |
| Asymmetry | 1.34 | 0.26 | 0.79 | 0.05 | 0.04 | 0.55 | -0.11 | 0.59 | -0.05 | -0.12 |
| Kurtosis | 17.82 | 5.91 | 15.83 | 4.83 | 4.33 | 9.73 | 8.21 | 9.03 | 6.65 | 7.12 |

**Table 3 - Correlations of daily series of returns on main worldwide financial sector indices (March 30, 2009, to December 31, 2013. Data source: Bloomberg).**

| Correlation | | CNX Finance (India) | DAX All Bankx (Germany) | KBW Bank (USA) | IFNC (Brazil) | ASX 200 Financials (Australia) | CAC Financials (France) | BMV (Mexico) | NMX 8350 (U. K.) | TSX Financials (Canada) | Moscow Exchange Financial Index (Russia) |
|---|---|---|---|---|---|---|---|---|---|---|---|
| CNX Finance | (India) | 1.00 | 0.31 | 0.18 | 0.28 | 0.24 | 0.29 | 0.23 | 0.32 | 0.20 | 0.34 |
| DAX All Bankx | (Germany) | 0.31 | 1.00 | 0.48 | 0.45 | 0.29 | 0.88 | 0.56 | 0.73 | 0.53 | 0.54 |
| KBW Bank | (USA) | 0.18 | 0.48 | 1.00 | 0.50 | 0.14 | 0.50 | 0.68 | 0.48 | 0.69 | 0.34 |
| IFNC | (Brazil) | 0.28 | 0.45 | 0.50 | 1.00 | 0.19 | 0.47 | 0.51 | 0.46 | 0.52 | 0.37 |
| ASX 200 F. | (Australia) | 0.24 | 0.29 | 0.14 | 0.19 | 1.00 | 0.34 | 0.21 | 0.29 | 0.24 | 0.26 |
| CAC F. | (France) | 0.29 | 0.88 | 0.50 | 0.47 | 0.34 | 1.00 | 0.58 | 0.77 | 0.55 | 0.52 |
| BMV | (Mexico) | 0.23 | 0.56 | 0.68 | 0.51 | 0.21 | 0.58 | 1.00 | 0.53 | 0.58 | 0.37 |
| NMX 8350 | (U. K.) | 0.32 | 0.73 | 0.48 | 0.46 | 0.29 | 0.77 | 0.53 | 1.00 | 0.50 | 0.49 |
| TSX Financials | (Canada) | 0.20 | 0.53 | 0.69 | 0.52 | 0.24 | 0.55 | 0.58 | 0.50 | 1.00 | 0.41 |
| Moscow E. F. I. | (Russia) | 0.34 | 0.54 | 0.34 | 0.37 | 0.26 | 0.52 | 0.37 | 0.49 | 0.41 | 1.00 |

We also apply Jarque and Bera (1981) test and the result suggests the rejection of the null hypothesis of normality at the 1% significance level for all indices. We propose ranking probability distribution functions considering a range with over 60 distributions, based on the metric proposed by Anderson and Darling (1952). Some of the best-ranked distributions are Johnson SU, Error, Hyperbolic Secant, and Laplace. Aiming to evidence the stationary or not of these time series, we perform the unit root test proposed by Dickey and Fuller (1979), in its augmented version (ADF test). Based on such a test, there is no unit root at the level of significance of 1%. We also use the ARCH–LM test proposed by Engle (1982) and find that at a 1% level of significance, eight series reject the null hypothesis of homoscedasticity, and at 10% of significance level, and no series seems to be homoscedastic. These results are not reported here for the sake of space, but they are available upon request.

### *3.2. Wavelet Power Spectrum*

Figure 2 exhibits the heat-maps of each normalized wavelet power spectrum, the colors ranges from blue (denoting low power/volatility) to red (high power/volatility). The region that suffers from boundary effects is denoted by the cone of influence (COI), which was drawn by a parabola-like black line that crossing over the heat map. Since that the normalized power spectrum of a white noise process converges to chi-squared distribution (Torrence and Compo, 1998), the significance statistics of time-frequency pairs of normalized wavelet power spectrums are tested against a AR (1) spectrum. The regions statistically significant on 5% are denoted with a black contour.

More pronounced episodes of high power and statistically significant were found at shorter periods within the band of 8 – 32 days. Most countries show spikes around 32-64 days band, and someone's cases of high volatility for lower frequencies (64-256 days) were found too.

For the European countries, the variance (at frequency 8 – 32 days) was concentrated between June 2011 and March 2012, there were too peaks of statistically significant power for Germany and France at longer frequency (128 – 256 days) during the interval. These results probably are related

with the fear of contagion effects by sovereign debt crisis, it's rose the risk aversion especially for the banking sector on Eurozone.

United States and Canada shares statistically significant regions in the beginning of the sample (March 2009 – September 2009) at shorter scales (8 – 32 days), the first one also had high variability at 64-128 days band from June 2009-September 2009, while the wavelet power spectrum reached a peak at 32-64 days band for the former. Weaker signals of high power were found for Mexico in the same interval, without any significant region of power for medium and lower frequencies. The volatility rose in the three countries between June 2011-January 2012 at shorter periods (more pronounced regions were found for Mexico), both Mexico and United shared too high and statistically significant power at 32-64 days band.

The Brics countries in the sample (Brazil, India, and Russia) had many high-power regions at shorter periods distributed between the whole-time intervals. This trend was stronger for Brazil, with spikes episodes statistically significant in every year. Looking at Australia, we conclude that power distribution is close with United States pattern, but without high variance for lower frequencies (more than 64 days).

As, theoretically, the response of these banking indices to external adverse disturbances has associated to increases in volatility levels, we will examine the co-movements across the markets on areas where the returns exhibited high variance. Since the majority of the volatility of international banking returns occurs at frequencies of periods shorter than 256 days, we will discard cycles longer than it in the rest of the paper. By the pattern discussed above, we will denote short-lived cycles for oscillations with frequency between 8 and 32 days, medium-lived cycles for fluctuations between 32~64 days bands and long-lived cycles to movements between 64~256 days.

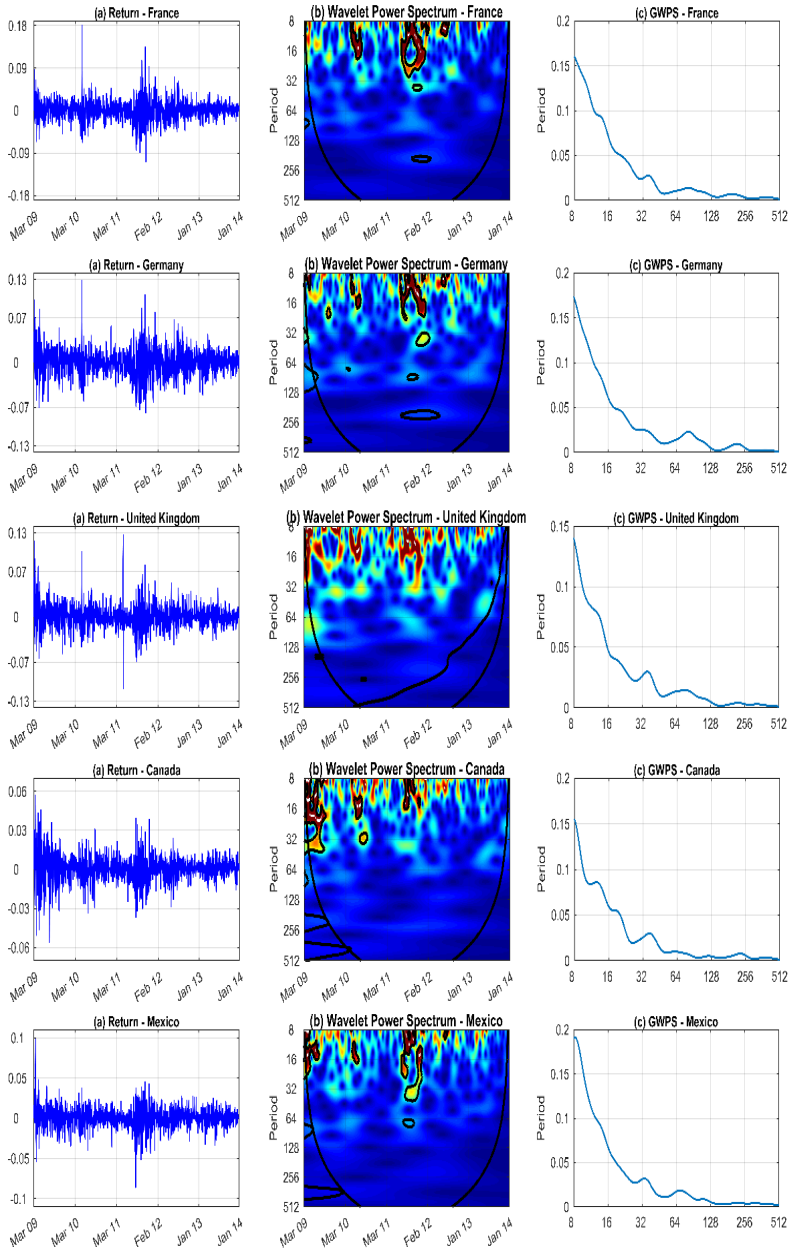


**Fig. 2 - Wavelet Power Spectrum on main worldwide financial sector indices a,b**

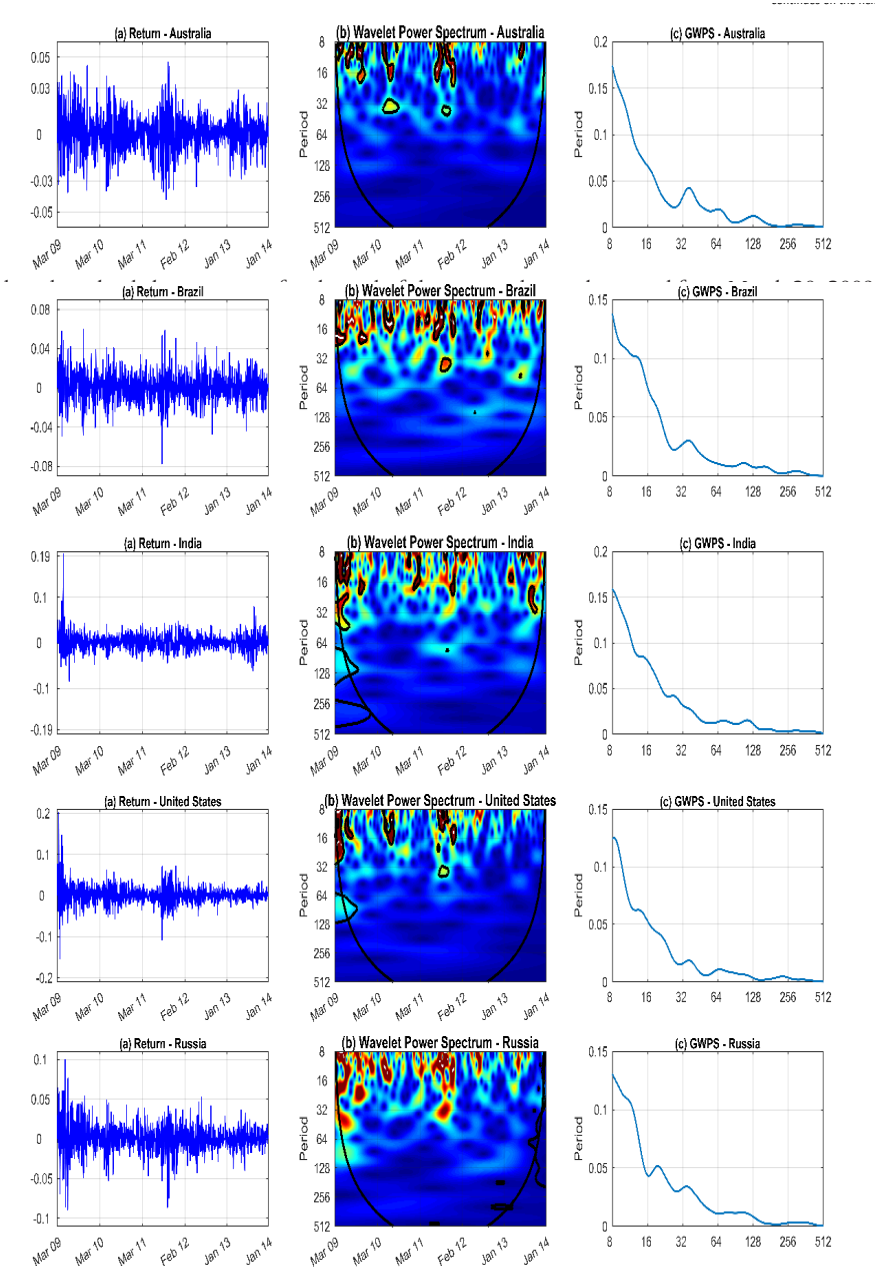


**Fig. 2 - Wavelet Power Spectrum on main worldwide financial sector indices [a,b]**

[a] This figure plots the nominal net return on financial sector index in terms of the local investor´s currency, based on the daily time series for the end-of-day quote, during the period from March 30, 2009, to December 31, 2013. [b] Data source: Bloomberg.

### *3.3. Business cycle dissimilarities*

In Figure 3, we plot the pairwise dissimilarity index based on the comparison between the wavelet transforms of the returns for each financial sector index. To compute the SVD of each pairwise of countries we set the range of frequencies between 8 and 256 days and the number of voices per octave was 25, which provide us a total of 126 scales ranging from 8 days up to 256 days. As discussed before, the dissimilarities compute the relationship between the wavelet spectra considering both the real and imaginary part, because the measure is based in the Hermitian angle, the value of the distance oscillates between 0 and $\frac{\pi}{2}$. Hence, two banking indices share the same high-power regions and that their phases are aligned. In other words, the contribution of cycles at each frequency to the total variance is similar between both countries and this contribution happens at the same time in both countries. We may also infer that the ups and downs of each cycle occur simultaneously in both countries.

To test the null hypothesis that a pairwise dissimilarity index is not synchronized we follow Aguiar-Conraria and Soares (2011) to fit an ARMA (1,1) model to build new samples by Monte Carlo methods (5000 simulations) and drawing errors from a Gaussian distribution, with the same variance as the estimated error terms.

Following Camacho et al. (2006), we convert the $(nxn)$ dissimilarity matrix to a $(nx2)$ matrix that contains the position of each banking index in two orthogonal axes.[2] In panel (a) we present the multidimensional scaling map and in panel (b) we present the cluster analysis by the dendogram. Both panels indicate a main group formed by the European countries (especially by France and Germany). Mexico and United States form the core group for America, with Canada sharing some alignment with them. On other hand, the Brics countries are far way one each other, denoting weak financial integration between them. In addition, the Australian banking index is other country that does not share synchronization with the "core" cycles.

[2] The transformation allows the dissimilarities were represented in a small number of dimensions that preserves, approximately, the original values (for technical details, see Timm, 2002 and Camacho et al. 2006).

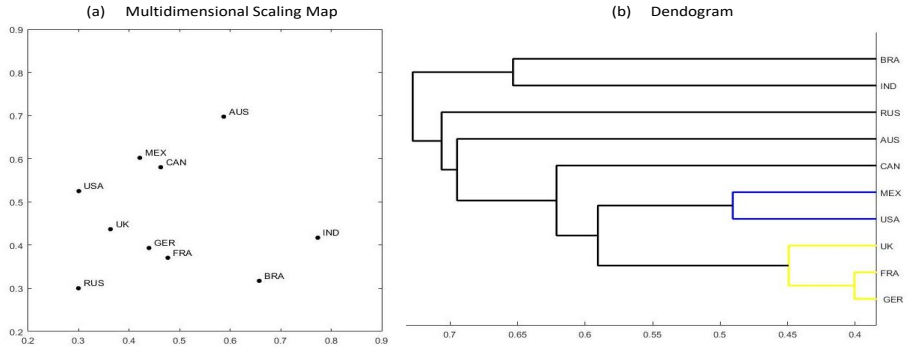


**Fig. 3 - Banking cycles dissimilarity of returns on main worldwide financial sector indices (March 30, 2009, to December 31, 2013).**

Aiming to assess if the pairwise synchronization is statistically significant at 5%, we follow this literature by relying on Monte Carlo simulations (1000 times). First, corroborating the Figure 2 and the average dissimilarities, Australia and Russia have banking cycles that seem to be independent of other banking systems; they are not synchronized with any other country at 5%. This inference also enables us to identify two intuitive blocs: a European core, based on the strong and significant synchronization between France, Germany, and United Kingdom and a strong synchronization between Canada, the United States, and Mexico, precisely the countries that comprise the North American Free Trade Agreement (NAFTA). The United Kingdom is also synchronized with each country of this trade bloc, and the same holds for France, except for the USA. Concerning emerging economies, Brazilian and Indian banking systems are also synchronized, likely because they belong to the BRIC trade bloc. We revisit this relationship discussion on synchronization and trade blocs, by analyzing multivariate coherency (subsection 4.2).

### *3.4. Preliminary analysis*

These previous findings suggest an apparent importance of the physical distance on the probability of high co-movement between financial sector indices. As NAFTA and especially Eurozone are trading blocs, the commercial channel is other possibility for pass through of disturbances.

Due to this evident pattern, in this subsection we suggest a simple analysis relating these variables. In the upper triangle of Table 4, we report information on the physical distance between the cities where the respective stock exchanges are located (in km), while in the lower triangle of Table 4, we can find countries dissimilarities, computed with the formula (5) with the whole dataset, March 30, 2009, to December 31, 2013. In Table 5, the difference is that we report in the upper triangle the trade balance, i.e. exports plus imports between partner countries (in U$$ bi), instead of physical distance. According to the dissimilarities reported in Table 4, the most dissimilar in Australia, with an average higher than 0.547, while the other average dissimilarities for each country range from 0.404 (France) to 0.512 (India). In terms of cross-partner volatility, Australia is the country with more homogeneous dissimilarities, while Germany has more volatile dissimilarities. Australia also has the highest dissimilarities, 0.651 concerning India and 0.588 with regards to Russia. The tighter pair of banking indices is USA and Mexico (0.245), followed by Germany and France (0.249).

Observing the physical distance between the cities where the respective stock exchanges are located, banking cycle synchronization does not seem to be independent of geographical issues, based on the significative correlation of 0.607, as well as some common patterns for both metrics of distance/difference. The city with the longest average distance concerning the others is Sidney, with more than 14,500 km, while the two cities with the least average distance are London and Paris, 7,89 and 7,154 respectively, the same pattern evidenced based on the dissimilarities. This finding is aligned to Aguiar-Conraria and Soares (2011), according to which the correlation between physical distance and dissimilarity based on industrial production for European countries is 0.67.

We also compare synchronization with trade between each pairwise of countries (Table 5). Once more, we find a significant correlation, -0.518. The negative sign is intuitive if we assume that commercial ties are useful to understand bank contagion, in the direction that stronger ties suggest lower dissimilarities. In addition to having the highest average dissimilarity and average physical distance, Australia has the lowest volume of foreign trade. USA, Germany, and Canada have the highest average volumes in this order, and they are among the countries with the lowest dissimilarities concerning the others. Analyzing each pair of foreign trade volumes, US commercial relations with Canada and Mexico are of the order of twice the relations between France and Germany, for example. Following, we highlight the strong German trade relations with the UK and the USA.

We summarize this finding by plotting in Figure 3 (a), the dispersion between physical distance in km (horizontal axis) and dissimilarity (vertical axis) and in Figure 3 (b) the dispersion between trade balance in US$ bi (horizontal axis) and dissimilarity (vertical axis). Finally, aiming to add to this discussion on the factors useful to better understand the 45 possible dissimilarities reported here, we follow Dimic et al. (2016) and Lin et al. (2018), by proposing a simple regression to measure the impact of related variables on wavelet coherency. We use the respective physical distance in km and trade balance in US$ bi and the results are reported below (regression 9):

$$diss_{i,j} = 0.4016 + 8.58 \times 10^{-6} \times phydist_{i,j} - 4.92 \times 10^{-5} \times trade_{i,j} \quad (9)$$

We find individual significance at 1% for the intercept and the parameter related to distance, and at 5% for the parameter related to trade, in the direction predicted by the associated fundamentals. These OLS estimation significance are robust in relation to using or not the covariance matrix a la Newey-West. We also find a joint significance and the explanatory power of this simple framework is higher than 0.407.

**Table 4 - Banking cycles dissimilarities of returns on main worldwide financial sector indices, lower triangle, and the physical distance between the cities where the respective stock exchanges are located (in km), upper triangle. (* *p-value* <0.05)**

| Dissimilarity | | CNX Finance | DAX All Bankx | KBW Bank | IFNC | ASX200 Financials | CAC Financials | BMV | NMX 8350 | TSX Financials | Moscow Exchange Financial Index |
|---|---|---|---|---|---|---|---|---|---|---|---|
| | | (India) | (Germany) | (USA) | (Brazil) | (Australia) | (France) | (Mexico) | (U. K.) | (Canada) | (Russia) |
| CNX Finance | (India) | | 6570 | 12537 | 13773 | 10156 | 7009 | 15645 | 7191 | 12488 | 5028 |
| DAX All Bankx | (Germany) | 0.536 | | 6202 | 9829 | 16482 | 478 | 9559 | 638 | 6333 | 2021 |
| KBW Bank | (USA) | 0.484 | 0.480 | | 7685 | 15988 | 5837 | 3359 | 5570 | 550 | 7510 |
| IFNC | (Brazil) | **0.398*** | 0.507 | 0.491 | | 13357 | 9401 | 7432 | 9470 | 8186 | 11806 |
| ASX 200 F. | (Australia) | 0.651 | 0.516 | 0.561 | 0.548 | | 16960 | 12972 | 16993 | 15567 | 14495 |
| CAC F. | (France) | 0.469 | **0.249*** | 0.444 | **0.406*** | 0.527 | | 9196 | 344 | 6000 | 2486 |
| BMV | (Mexico) | 0.493 | 0.420 | **0.245*** | 0.524 | 0.516 | **0.393*** | | 8928 | 3261 | 10719 |
| NMX 8350 | (U. K.) | 0.541 | **0.324*** | **0.385*** | 0.563 | 0.468 | **0.275*** | **0.386*** | | 5712 | 2500 |
| TSX Financials | (Canada) | 0.495 | 0.521 | **0.377*** | 0.518 | 0.552 | **0.414*** | **0.347*** | **0.360*** | | 7484 |
| Moscow E. F. I. | (Russia) | 0.545 | 0.454 | 0.453 | 0.538 | 0.588 | 0.456 | 0.472 | 0.428 | 0.472 | |

**Table 5 - Banking cycles dissimilarities of returns on main worldwide financial sector indices, lower triangle, and the trade balance – exports, FOB to partner countries + imports, CIF from partner countries between the countries in U$$ bi, upper triangle. (* *p-value* <0.05)**

| Dissimilarity | | CNX Finance | DAX All Bankx | KBW Bank | IFNC | ASX200 Financials | CAC Financials | BMV | NMX 8350 | TSX Financials | Moscow Exchange Financial Index |
|---|---|---|---|---|---|---|---|---|---|---|---|
| | | (India) | (Germany) | (USA) | (Brazil) | (Australia) | (France) | (Mexico) | (U. K.) | (Canada) | (Russia) |
| CNX Finance | (India) | | 101 | 265 | 43 | 73 | 44 | 21 | 72 | 23 | 34 |
| DAX All Bankx | (Germany) | 0.536 | | 720 | 109 | 65 | 1067 | 78 | 646 | 78 | 357 |
| KBW Bank | (USA) | 0.484 | 0.480 | | 301 | 172 | 334 | 2151 | 512 | 550 | 150 |
| IFNC | (Brazil) | **0.398*** | 0.507 | 0.491 | | 9 | 47 | 44 | 40 | 29 | 29 |
| ASX 200 F. | (Australia) | 0.651 | 0.516 | 0.561 | 0.548 | | 27 | 10 | 62 | 17 | 6 |
| CAC F. | (France) | 0.469 | **0.249*** | 0.444 | **0.406*** | 0.527 | | 20 | 337 | 38 | 109 |
| BMV | (Mexico) | 0.493 | 0.420 | **0.245*** | 0.524 | 0.516 | **0.393*** | | 20 | 122 | 6 |
| NMX 8350 | (U. K.) | 0.541 | **0.324*** | **0.385*** | 0.563 | 0.468 | **0.275*** | **0.386*** | | 118 | 84 |
| TSX Financials | (Canada) | 0.495 | 0.521 | **0.377*** | 0.518 | 0.552 | **0.414*** | **0.347*** | **0.360*** | | 12 |
| Moscow E. F. I. | (Russia) | 0.545 | 0.454 | 0.453 | 0.538 | 0.588 | 0.456 | 0.472 | 0.428 | 0.472 | |

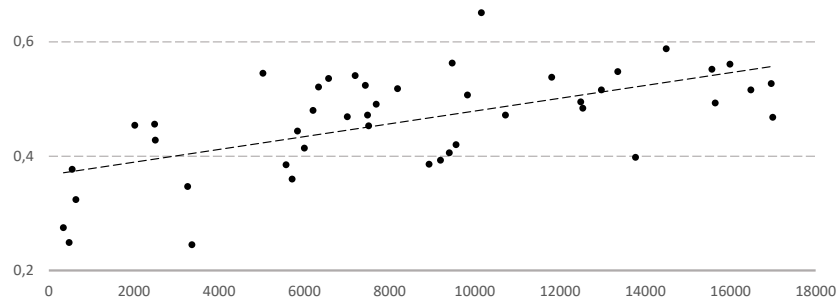


a) The dispersion between physical distance in km (horizontal axis) and dissimilarity (vertical axis)

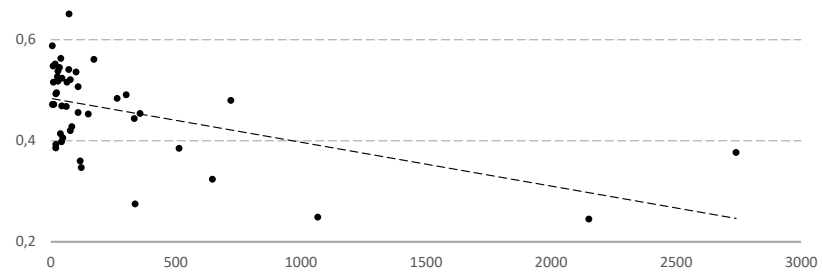


b) The dispersion between trade balance in US$ bi (horizontal axis) and dissimilarity (vertical axis)

Fig. 3. The dispersion between dissimilarity vs trade and physical distance a, b, c

[a] Banking cycle dissimilarity of returns on main worldwide financial sector indices (March 30, 2009, to December 31, 2013). [b] Physical distance between the cities where the respective stock exchanges are located. [c] Trade balance – exports, FOB to partner countries + imports, CIF from partner countries between the countries in U$$ bi, from 2009:2 to 2013:4.

## 4. Empirical exercise

### *4.1. Wavelet phase difference and cross-wavelets*

In this section, we present our main empirical results.

To assess the unconditional local correlation between the banking sector indices and to examine the delay between the same we estimate the wavelet coherency and the phase-difference, respectively. The significance of coherency is obtained by the same method of the dissimilarity pairwise, performing Monte-Carlo simulations and extracting critical values by an ARMA (1,1) model to each of the series. How the phases are angular measures (Zar, 1996), to compute the critical values of the phase-difference, first we compute the average phase difference within the short-lived cycles (8∼32 days), medium-lived cycles (32∼64 days) and long-lived cycles (64∼256 days) and then the confidence intervals are computed by consider values as extreme as two endpoints of the confidence interval for the circular mean at each point in time. For wavelet coherency the 5% significance level region is identified with a black contour and for phase difference the limits of the confidence intervals are drawn with black dashed lines.

We follow the same procedure for all 45 pairwise available, given 10 banking indices used here: we plot the wavelet coherency on the left and phase-difference on the right. Concerning the coherency, it ranges from low coherency in blue to high coherency in red and the respective cone of influence is shown with a black line, designating the 5% significance level. Concerning the phase-difference, we also plot it with plus and minus two standard deviations. In this subsection, we discuss the countries that we have identified as belonging to a bloc or group, based on the previous finding.

In Figure 4, we plot both frameworks for the European core: France, Germany, and the United Kingdom. Concerning up to 8∼32 days frequency-band, France exhibits many points and successive regions of high coherency with Germany and the UK during almost the entire period.

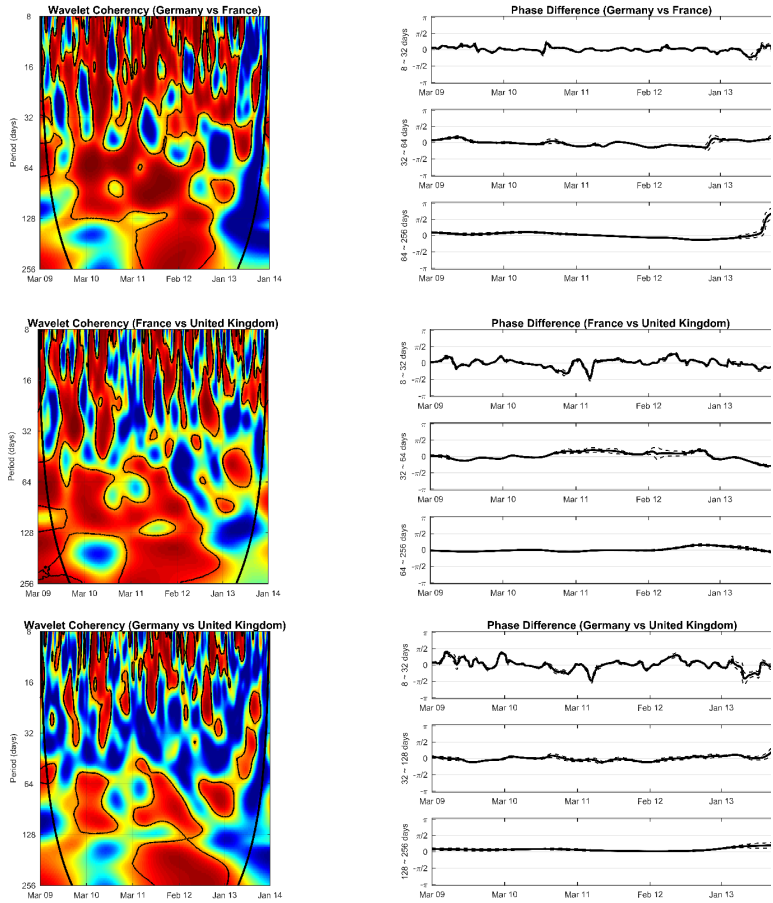


**Fig. 4- European core: wavelet coherency (on the left) and phase-difference (on the right).** [a,b]

[a] The coherency ranges from low (blue) to high (red) values and the respective cone of influence is shown with a black line, designating the 5% significance level. [b] We also plot the phase-difference with plus and minus two standard deviations.

We find a somewhat similar pattern for the UK and Germany, but with less intensity. Between 2010 and 2013 Germany and France exhibits strong coherency at medium-lived cycles (32~64 days), after the first quarter of 2011 the phase-difference analysis indicates that France leads the Germany cycle in some intervals. When we look at long-term frequency (64~256 days) we observe a big area of high coherency between the fourth quarter of 2009 until 2012, again France has been leading

the Germany fluctuations during 2012. The France has been leading the United Kingdom cycle for medium-term cycle between the aftermath of 2010 and 2012 and between 2012 for the long-lived cycle.

Concerning oscillations between 32∼64 days the estimates suggest small areas of coherency between Germany and United Kingdom, with one unique episode of significant region that covers the whole frequency band in 2013. At long term frequency, the countries share regular regions of strong coherency across the sample with phases completely aligned (phase-difference statistically equal zero). Finally, discarding the region affected by edge effects (COI), the banking indices moving in phase $\left[\phi_{xy} \in \left(-\frac{\pi}{2}, \frac{\pi}{2}\right)\right]$ across the whole sample for all frequencies. It's wort noting that similar results were find by Aguiar-Conraria and Soares (2011) for business cycle analysis, with Germany-France forming the core of Euro land and the former has been lagging the latter in cycles of long-term (4,5∼8 years).

Figure 5 reveals that co-movement between USA and Mexico changes over time-frequency domain. The wavelet coherence diagrams show local correlation at long-term for the period 2004Q2-2010Q3, the phase-difference are slightly higher than zero for the most of time, suggesting that USA banking sector is the source of oscillations on Mexican banking sector in aftermath of financial crises.

The following Euro sovereign debt crises period demarks a rising of high coherency between the countries from the medium-term cycles reaching the short-term cycles in the second quarter of 2011. The phase-difference relation between the countries is erratic around zero, indicating common response of the indices to adverse shocks at short-term. The American banking sector have big areas of high coherence with Canada only for medium-lived and long-lived cycles. Most of the strong co-movement begins in late of 2010 at long-term horizon and it spreads to 32∼128 days band since the second quarter of 2011 until the end of interval. It's worth noting a small area of high coherency at short-term frequency at the end of 2011. Looking the phase-difference into intervals of high coherency, it's clear that USA leads Canada for long-term frequencies and the opposite occurs for medium-term frequencies.

Moreover, there are regions of strong coherency between the high-frequency cycles only for the USA and Mexico in 2011. The American cycles for the one-month to six-month frequency-band have regions of strong

coherence in the beginning and at the end of the time with Canada and Mexico. With a frequency of six months or more, the cycles are coherent principally between Canada and the USA during the first half of the time and between Canada and Mexico in the second half. To summarize the lower frequency pattern, these economies of NAFTA bloc behave as if they were highly synchronized all the time and we find some isolated out of phase behavior with the other partners only for the Canadian higher frequency cycles.

Finally, Mexico and Canada show stable regions of coherency only at long-term frequencies. In the first area (2009Q2-2010Q2) it is Canada that leads the Mexican cycle, and in the second area (2011Q2-2013Q1) the phases are aligned.

Concerning emerging economies (Figure 6), there is a clear high coherency region until end-2010 at medium and long-term frequencies. The phases of both frequencies are equal to 0 most of period, indicating banking sectors highly synchronized. The convergence signals loses power in the second half of the sample, but we a relevant region of high coherency at long-term frequencies between 2011Q3-2012Q1 with the Brazilian cycle leading the Indian cycle. Other wavelet coherency maps and the respective phase-differences are not reported here, but they are available upon request.

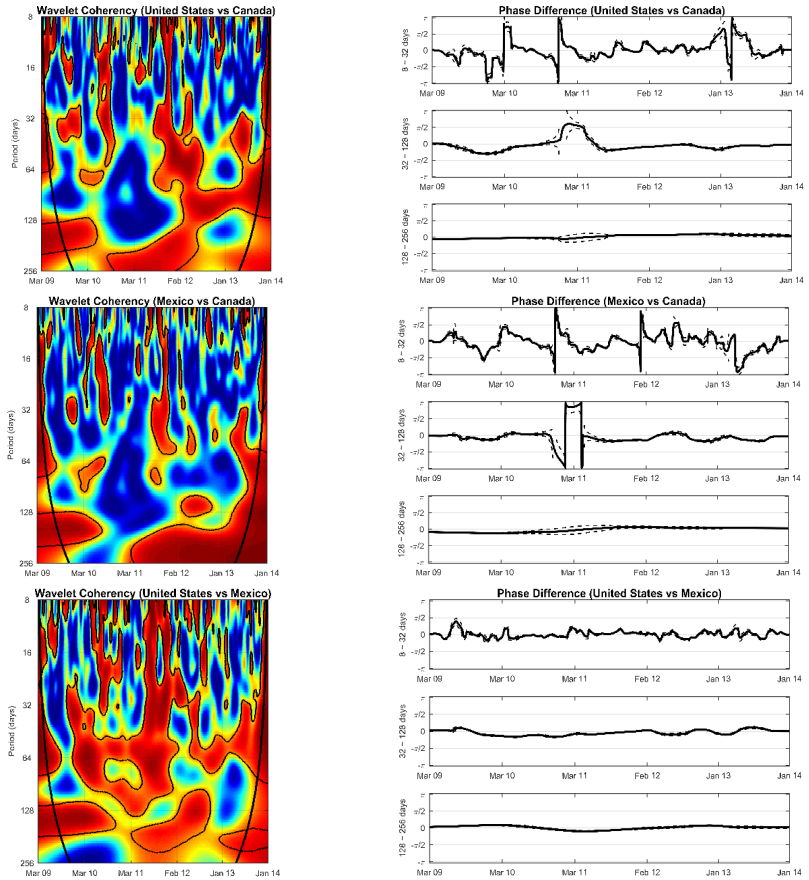


**Fig. 5 - NAFTA: wavelet coherency (on the left) and phase-difference (on the right).** [a,b]

[a] The coherency ranges from low (blue) to high (red) values and the respective cone of influence is shown with a black line, designating the 5% significance level. [b] We also plot the phase-difference with plus and minus two standard deviations.

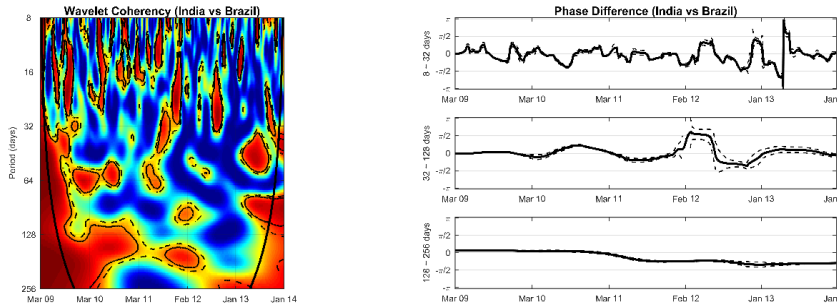


**Fig. 6 - India vs Brazil: wavelet coherency (on the left) and phase-difference (on the right).** [a,b]

[a] The coherency ranges from low (blue) to high (red) values and the respective cone of influence is shown with a black line, designating the 5% significance level. [b] We also plot the phase-difference with plus and minus two standard deviations.

## *4.2. Multivariate analysis*

In the previous subsection, we find out regions of strong coherency between NAFTA partners, as well as considering the European core: France, Germany, and the United Kingdom. Aiming to better understand the relationship in each of such blocs, we propose the use of the multiple coherence, partial coherence, as well as partial phase-difference and partial gain. The first one measures the degree of adjustment of the explanatory variables on the dependent variable in the time-frequency domain. The other measures calculate the relationship between the fluctuations of two markets, controlling the influence of a third party on the oscillations in the time-frequency space. According to Figure 7, the presence of successive areas with significance statistics in the multiple coherence denotes a good overall fit in the model, reporting that the Canadian and American financial indices are useful to explain Mexico's financial index in the time-frequency location.

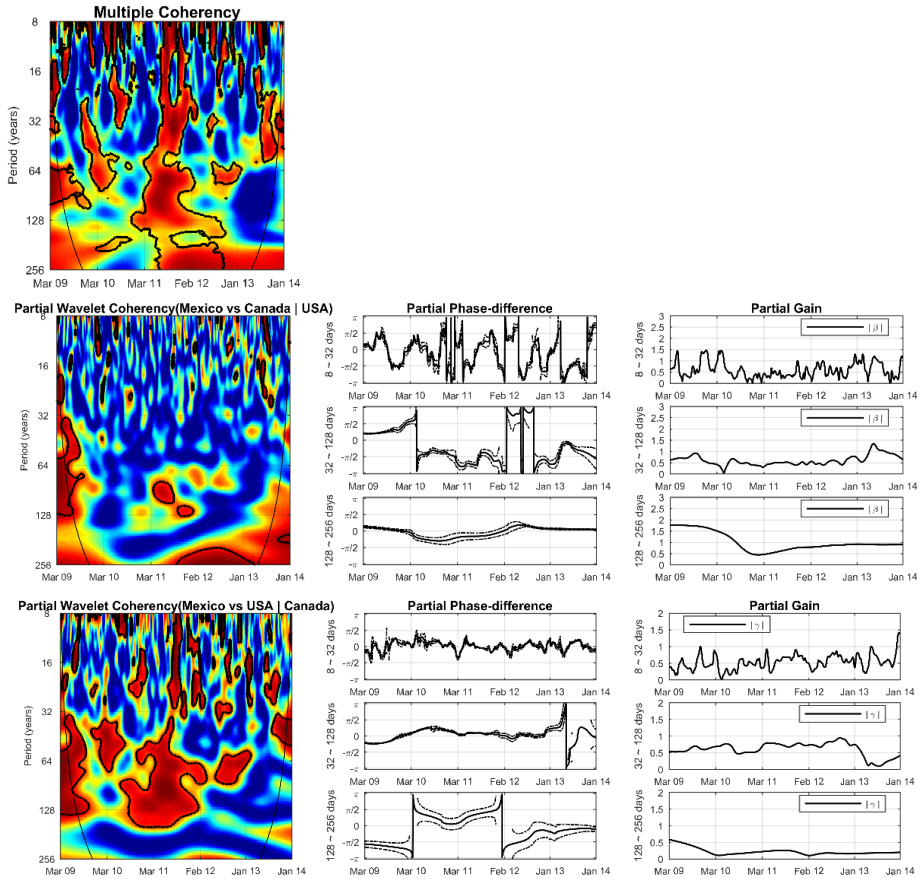


**Fig. 7 - NAFTA: joint wavelet coherency (on the left) and phase-difference (on the right).** [a,b]

[a] The coherency ranges from low (blue) to high (red) values and the respective cone of influence is shown with a black line, designating the 5% significance level. [b] We also plot the phase-difference with plus and minus two standard deviations.

In short-term (8~32 days) we find a regular pattern of absence of synchronization from the second quarter of 2011 to the first quarter of 2012. For mid-run frequencies (32 ~128 days), the multiple coherence is continuously significant from 2010 to 2013 in some locations. At the long-term horizon (128 ~256 days), the range of significant decreases to 2011 until the third quarter of 2012. Therefore, we can find a strong performance in the period 2010-2012 in all frequencies, characterized by greater uncertainties in the market due to the sovereign debt crisis in some European countries.

Controlling the effects of the US index, we highlight a broader decrease in significant coherency area between Mexico and Canada. The sovereign debt crisis period is correlated with a small area of high and significant coherence spanning 32~128 days. At long run frequency (128~256 days), the partial coherence is significant in a narrow area after the first quarter of 2011.

The partial coherence between Mexico and Canada is overall lower than the unconditional case. It shows greater coherence in the medium-term horizon, and absence of synchronization in the long term. In the short term, there is a region of coherence between the second half of 2011 and early 2012, the partial phase-difference is set to zero, indicates strong contemporaneous co-movements among the Countries. On the other hand, for long-term frequencies (0.5 ~ 1 year), the partial coherency is significant between 2010 and first-half of 2012, with Mexico leading Canada, but during 2011 the partial phase-difference is set to $(0, \pi/2)$ indicating a positive co-movement, and in the early of 2012 the partial phase-difference is located between $(-\pi, -\pi/2)$, and the index are out-phase.

The partial coherence between Mexico and USA repeats the pattern of the previous relationship, but with greater intensity in terms of synchronization. At higher frequencies (0.05 ~ 0.1 year), is predominant peaks with low duration from 2010-2012, the partial phase-difference are located in the interval $(-\pi/2, \pi/2)$, indicates a positive synchronization, with irregular pattern of leads and lags. At medium-term, the partial coherence is only significant at the range 2010 until the first-quarter of 2012, the US is leading in the interval (quarters 2011:2-2011:4). At that range, the partial gain (coefficient of regression) increased, reaching a value slightly below 1.0. For low frequencies band (0.5 ~ 1.0 year) the partial phase-difference indicated that US leads Mexico when partial coherence is significant (second-half of 2010), with the partial gains' coefficient above 0.5. In sum, US index anticipates fluctuations of the counterpart Mexican in the cycles of 0.1 ~ 0.3 year (medium frequency), and cycles of 0.5 ~ 1.0 year (long-term) during the period of instability in the market, with no contagion in another range.

Now, we analyze the multiple coherencies between France versus Germany and the UK (Figure 8).

There is a lack of high coherency in the short-term and we identify two regions with strong co-movements at a lower frequency. The first one covers

the period between the end of 2009 and the first half of 2010 (frequency band 0.65 ~ 1.2 years), while the most important covers the region of the year 2012 (frequency equal to or greater than 1 year). The medium-term banking cycles show statistical significance between the first and third quarter of 2010 (0.2 ~ 0.3 year), and a second period with weaker convergence in the year 2011.

The partial coherence between France and Germany (controlling for the UK) indicates three regions of strong coherence at the horizon of medium-term (quarters 2012: 2-2012: 3) and long-term (quarters 2010: 2 and 2010: 2 - 2012: 4). At medium-term, the cycles move in-phase, with Germany leading, and the partial gain increased during the range, getting close to 0.5 in the third quarter of 2012. At a frequency band located in 128 ~ 256 days, the first region statistically significant is associated with the partial phase-difference between $-\pi/2$ and 0 reporting again that Germany leads France, and the partial gain fluctuates slight of zero. On the other hand, during 2012: 2 - 2012: 4, Germany leads France, but they are out-phase, with the coefficient of regression below 0.5.

The partial coherence between France and the United Kingdom exhibits an important region of strong synchronization of long-term cycles after the beginning of 2010. More specifically, France leads the UK throughout the year 2011, while the UK is leading France from the second quarter of 2012 until the middle of 2013. In the last interval, the coefficient of partial gain increased, reaching a value close to unity in the first quarter of 2013. In other words, our results indicate strong co-movements between the series, with the cycle of UK contagious the France index. In the short and medium-term the statistically significant regions do not exceed one quarter, while the partial phase-difference presents an irregular pattern, which suggests the absence of synchronization.

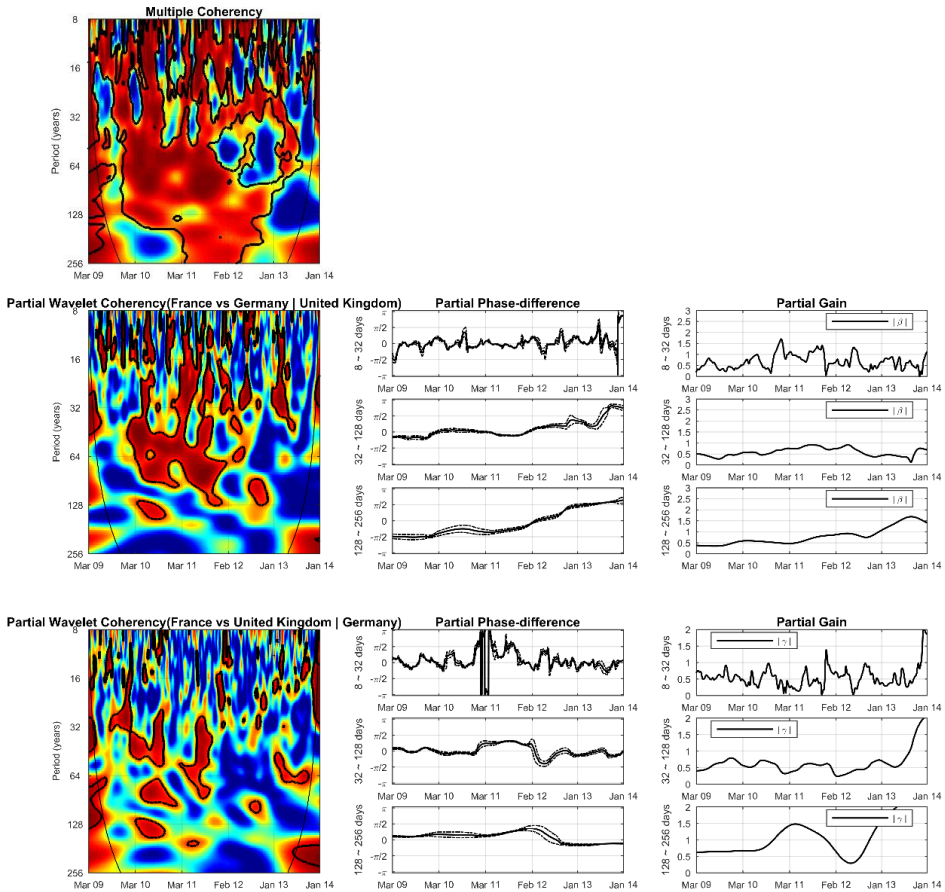


**Fig. 8. EURO core: joint wavelet coherency (on the left) and phase-difference (on the right).** [a,b]

[a] The coherency ranges from low (blue) to high (red) values and the respective cone of influence is shown with a black line, designating the 5% significance level. [b] We also plot the phase-difference with plus and minus two standard deviations.

## 5. Concluding remarks

Banking crises are costly, and a great deal of prudential effort is undertaken to avoid them. For instance, Bordo et al. (2001) estimate losses of around 6% of GDP associated with a banking crisis in the last quarter of the 20th century, while Laeven and Valencia (2013) report losses of about

30% of GDP during the last global financial crisis (2007–2009). According to OECD (2012), financial contagion shocks dramatically increase countries' risk of suffering a financial crisis: in periods where a country is not affected by financial contagion, its annual crisis probability is slightly above 1% but rises to more than 28% in periods when it is hit by a strong contagion shock.

Regardless of the cause of the shocks in the banking system – due to fraud and internal irregularities in an institution or a consequence of macro fundamentals –, the contagion effect of bank failure is seen by much of the literature on international finance as a relevant and worrying issue to be addressed. In practice, policymakers aim to avoid banking crises, and although they can to some extent control domestic conditions, internationally transmitted crises are difficult to tackle, which motivates banking crises as one of the main reasons for worldwide bank regulation mainly from the '80s. In this sense, Dungey and Gajurel (2015) claim that while policymakers and regulatory authorities are rightly concerned with the systematic transmission of banking crises, reducing the potential for idiosyncratic contagion can importantly reduce the consequences for the domestic economy. In other words, the systematic contagion effects present in these markets during this crisis could not have been reduced by further banking regulatory measures such as increased capital requirements. However, there is scope for further reduction in the probability of banking crises due to international linkages through idiosyncratic contagion.

Moreover, this literature on business cycle synchronization is usually related to the optimal currency areas because it is seen as a necessary condition: a country with an asynchronous business cycle must face difficulties in a monetary union. We claim that it is also relevant to relate cycle synchronization to discussion on trade, as a useful tool for a suggestion of admission of new commercial partners or even in evaluating the benefits of such commercial arrangements.

In this context of banking contagion among economies in a trade bloc, considering NAFTA, we find that the presence of successive areas with significance statistics in the multiple coherence denotes a good overall fit in the model, reporting that the Canadian and American financial indices are useful to explain Mexico's financial index in the time-frequency location. Controlling the effects of the US index, we highlight a broader decrease in significant coherency area between Mexico and Canada. The

partial coherence between Mexico and USA repeats the pattern of the previous relationship, but with greater intensity in terms of synchronization. In sum, US index anticipates fluctuations of the counterpart Mexican in the cycles of 0.1 ~ 0.3 year (medium frequency), and cycles of 0.5 ~ 1.0 year (long-term) during the period of instability in the market, with no contagion in another range.

Observing main Eurozone economies, the partial coherence between France and Germany (controlling for the UK) indicates three regions of strong coherence at the horizon of medium-term (quarters 2012: 2-2012: 3) and long-term (quarters 2010: 2 and 2010: 2 - 2012: 4), while the partial coherence between France and the United Kingdom exhibits an important region of strong synchronization of long-term cycles after the beginning of 2010, with the cycle of UK contagious the France index.

Here we claim that potentially there is a gain for regulators, researchers, and policymakers to consider the functioning of transmission of business cycles between each pair of banking systems or even considering a small group of countries. It seems useful to identify which banking system can act as a leader in the group of synchronized countries. In this context, our main findings can shed light on this discussion on business cycle synchronization and trade, as a useful tool for a suggestion of admission of new commercial partners or even in evaluating the benefits of such commercial arrangements.

## References

Aguiar-Conraria, L., Soares, M., 2010. The continuous wavelet transform: a primer. NIPE-WP 23/2010.

Aguiar-Conraria, L., Soares, M., 2011. Business cycle synchronization and the Euro: A wavelet analysis. Journal of Macroeconomics, 33, 477–489.'

Aguiar-Conraria, L., Soares, M., 2014. The continuous wavelet transform: moving beyond uni-and bivariate analysis. Journal of Econonomic Survey, 28, 344–375.

Aguiar-Conraria, L., Martins, M, Soares, M., 2018. Estimating the Taylor rule in the time-frequency domain. Journal of Macroeconomics, 57, 122–137.

Aharony, J., Swary, I., 1983. Contagion Effects of Bank Failures: Evidence from Capital Markets. The Journal of Business, 56, 305–322.

Akhtaruzzaman, M., Boubaker, S., & Sensoy, A. (2021). Financial contagion during COVID–19 crisis. Finance Research Letters, 38, 101604.

Anderson, T., Darling, D., 1952. Asymptotic theory of certain goodness-of-fit criteria based on stochastic processes. *Annals of Mathematical Statistics*, 23, 193–212.

Beveridge, S., Nelson, C., 1981. A new approach to decomposition of economic Time series into permanent and transitory Components with particular attention to Measurement of the business cycle. Journal of Monetary Economics, 7, 151–174.

Bordo, M., Eichengreen, B., Klingebiel, D., Martinez-Peria, M.S., 2001. Is the crisis problem growing more severe? Economic Policy, 16, 51–82.

Bühler, W., & Prokopczuk, M., 2010. Systemic risk: Is the banking sector special?. Available at SSRN 1612683.

Dickey, D., Wayne, F., 1979. Likelihood ratio statistics for autoregressive time series with a unit root. Econometrica, 49, 1057–1072.

Diebold, F. X., & Yilmaz, K. (2012). Better to give than to receive: Predictive directional measurement of volatility spillovers. International Journal of forecasting, 28(1), 57-66.

Dimic, N., Kiviaho, J. Piljak, V., Aijo, J., 2016. Impact of financial market uncertainty and macroeconomic factors on stock–bond correlation in emerging markets. Research in International Business and Finance, 36, 41–51.

Dungey, M., Gajurel, D., 2015. Contagion and banking crisis – International evidence for 2007–2009. Journal of Banking & Finance, 60, 271–283.

Engle, R., 1982. Autoregressive Conditional Heteroscedasticity with Estimates of the Variance of United Kingdom Inflation. Econometrica, 50, 987–1007.

Farge, M. (1992). Wavelet transforms and their applications to turbulence. Annual review of fluid mechanics, 24(1), 395-458.

Gamba-Santamaria, S., Gomez-Gonzalez, J. E., Hurtado-Guarin, J. L., & Melo-Velandia, L. F. (2017). Stock market volatility spillovers: Evidence for Latin America. Finance Research Letters, 20, 207-216.

Gençay, R., Selçuk, F., & Whitcher, B. (2001). Differentiating intraday seasonalities through wavelet multi-scaling. Physica A: Statistical Mechanics and its Applications, 289(3-4), 543-556.

Goupillaud, P., Grossman, A., Morlet, J., 1984. Cycle-octave and related transforms in seismic signal analysis. Geoexploration 23, 85–102.

Grossmann, A., Morlet, J., 1984. Decomposition of Hardy functions into square integrable wavelets of constant shape. SIAM Journal on Mathematical Analysis 15, 723–736.

Hung, N. T. (2019). Spillover effects between stock prices and exchange rates for the central and eastern European countries. Global Business Review, 0972150919869772.

In, F. & Kim, S. (2013). An introduction to wavelet theory in finance: a wavelet multiscale approach. World scientific.

Jarque, C., Bera, A., 1981. Efficient tests f or normality, homoscedasticity and serial independence of regression residuals: Monte Carlo evidence. Economics Letters, 7, 313–318.

Kaminsky, G. L., & Reinhart, C. M. (2000). On crises, contagion, and confusion. Journal of international Economics, 51(1), 145-168.

Kaminsky, G. L., & Reinhart, C. M. (2002). Financial markets in times of stress. Journal of Development Economics, 69(2), 451-470.

Kaufman, G. G. (1992). Bank contagion: theory and evidence (No. 92-13). Federal Reserve Bank of Chicago.

Jung, R. C., & Maderitsch, R. (2014). Structural breaks in volatility spillovers between international financial markets: Contagion or mere interdependence? Journal of Banking & Finance, 47, 331-342.

Laeven, L., Valencia, F., 2013. Systemic banking crises database. IMF Economic Review, 61, 225–270.

Lilly, J. M., & Olhede, S. C. (2009). Bivariate instantaneous frequency and bandwidth. IEEE Transactions on Signal Processing, 58(2), 591-603.

Lin, F., Yang, S., Marsh, T., Chen, Y., 2018. Stock and bond return relations and stock market uncertainty: Evidence from wavelet analysis. International Review of Economics and Finance, 55, 285–294.

Loh, L., 2013. Co-movement of Asia-Pacific with European and US stock market returns: A cross-time-frequency analysis. Research in International Business and Finance, 29, 1–13.

Matos, P., Benegas., Costa, H., 2019. Chaos in the world banking system? Working paper CAEN/UFC.

Matos, P., Costa, A., da Silva, C. 2021. On the Risk-based Contagion of G7 Banking System and the COVID-19 Pandemic. Global Business Review, online version, 1 – 21.

Matos, P., Oquendo, R., Trompieri, N., 2016. Integration and contagion of BRIC financial markets. Journal of Applied Economics and Business, 4, 23–48.

Mandler, M., Scharnagl, M. 2019. Financial cycles across G7 economies: A view from wavelet analysis, Deutsche Bundesbank Discussion Paper 22/2019.

Meltzer, A., 1967. Major issues in the regulation of financial institutions. Journal of Political Economy, 75, 482-501.

Pavlova, A., & Rigobon, R. (2008). The role of portfolio constraints in the international propagation of shocks. The Review of Economic Studies, 75(4), 1215-1256.

OECD, 2012. Financial Contagion in the Era of Globalised Banking? OECD Economics Department Policy Notes, No. 14, June.

Rajwani, S., & Kumar, D. (2016). Asymmetric dynamic conditional correlation approach to financial contagion: a study of Asian markets. Global Business Review, 17, 1339-1356.

Rajwani, S., & Kumar, D. (2019). Measuring Dependence Between the USA and the Asian Economies: A Time-varying Copula Approach. Global Business Review, 20, 962-980.

Rigobon, R. (2019). Contagion, Spillover, and Interdependence. Economía, 19(2), 69-100.

Rua, A., Nunes, L., 2009. International comovement of stock market returns: A wavelet analysis. Journal of Empirical Finance, 16, 632–639.

Scharnagl, M., Mandler, M. 2019. Real and financial cycles in euro area economies: Results from wavelet analysis, Journal of Economics and Statistics, 239(5-6), 895-916.

Torrence, C., Compo., G.P. (1998). A Practical Guide to Wavelet Analysis. Bulletin of the American Meteorological Society, 79, 61–78.

Torrence, C., & Webster, P. J. (1999). Interdecadal changes in the ENSO–monsoon system. Journal of climate, 12(8), 2679-2690.